Atmos. Chem. Phys. Discuss., 14, 8063–8094, 2014
www.atmos-chem-phys-discuss.net/14/8063/2014/
doi:10.5194/acpd-14-8063-2014

Atmospheric Chemistry and Physics Discussions
Open Access

A new parameterization of dust dry deposition over rough surfaces

J. Zhang[1,2] and Y. Shao[2]

[1]Key Laboratory of Mechanics on Disaster and Environment in Western China, Lanzhou University, 730000 Lanzhou, China
[2]Institute for Geophysics and Meteorology, University of Cologne, 50937 Cologne, Germany

Received: 6 January 2014 – Accepted: 22 February 2014 – Published: 25 March 2014

Correspondence to: J. Zhang (zhang-j@lzu.edu.cn)

Published by Copernicus Publications on behalf of the European Geosciences Union.

ACPD
14, 8063–8094, 2014

A new parameterization of dust dry deposition over rough surfaces

J. Zhang and Y. Shao

Abstract

The performances of existing dust dry deposition schemes are rather unsatisfactory for rough surfaces. In this study, we propose a new scheme to overcome some of the deficiencies. The scheme takes into consideration of the impacts of roughness elements on turbulent dust diffusion and surface dust collection. A relationship between the aerodynamics and surface collection process is established by using an analogy between deposition-flux partition and drag partition. The scheme is then tested against a wind-tunnel dataset for four different surfaces and a good agreement between the scheme predictions and the observations is found. The sensitivity of the scheme to the input parameters is tested. Important factors which affect dust deposition in different particle size ranges are identified. The scheme shows good capacity for modeling dust deposition over rough surfaces.

1 Introduction

Dust dry deposition, the removal of dust from the atmosphere onto the surface in the absence of precipitation, can be divided into several sub-processes, including turbulence diffusion, surface collection and gravitational settling (Droppo, 2006). To estimate dust deposition flux in terms of dust concentration, the method of deposition velocity (or its inverses, the resistance) is widely used (Sehmel, 1980; Slinn, 1982; Hicks et al., 1987; Wesely and Hicks, 2000; Raupach et al., 2001; Zhang et al., 2001; Petroff and Zhang, 2010; Seinfeld and Pandis, 2012; Kouznetsov and Sofiev, 2012). The effects of the sub-processes are represented with the corresponding resistances, i.e. turbulence diffusion, surface collection and gravitational settling are respectively related to aerodynamic resistance, surface resistance and gravitational resistance. Deposition velocity, defined as the ratio of dust deposition flux and dust concentration is a quantity which describes the joint effect of the above mentioned resistances.

Deposition velocity is a key quantity used in dust deposition parameterizations. The approach is in analogy to electrical circuits: deposition velocity is considered to be the inverse of the deposition resistance which comprises the contributions of the aerodynamic and surface resistances in series and the gravitational resistance in parallel (Hicks et al., 1987; Seinfeld and Pandis, 2012). Slinn (1982) deduced an analytical expression for dust deposition velocity over canopy surface based on the dust concentration equation. In his approach, the gravitational effect was not considered at first but then directly added to the result.

The existing deposition-velocity approach has two deficits. First, while the gravitational resistance is often treated as a resistance in parallel to the turbulent diffusion resistance, gravitational settling is not driven by concentration gradient and the settling process cannot be expressed in an electrical-circuit analogy. More specifically, the usual treatment of gravitational settling as a parallel resistance (Slinn, 1982; Zhang et al., 2001; Petroff and Zhang, 2010), including the modified version of Seinfeld and Pandis (2012), does not satisfy the dust mass conservation requirement (Venkatram and Pleim, 1999). Second, the collection of particles by the surface is normally described based on the studies of dust deposition on isolated collectors (Petroff et al., 2008). Kouznetsov and Sofiev (2012) reported a more detailed scheme, but the "collection scale" they introduced does not have a clear physical interpretation and is thus practically difficult to determine. In dust deposition schemes, the typical size of the surface collectors is often the only parameter used for the characterization of the surface, which is insufficient for rough surfaces.

The deficiencies of the existing dust deposition schemes are clearly revealed in our recent comparison of the Slinn and Slinn (1980, SS80 hereafter) and Slinn (1982, S82 hereafter) with the wind-tunnel observations, as described in the companion paper by Zhang et al. (2014). The results of the latter study are summarized in Fig. 1 which shows that the SS80 and S82 schemes work well for smooth surfaces (such as wood surface) but perform rather poorly for rough surfaces (e.g. surface with trees). By tuning

ACPD
14, 8063–8094, 2014

some input parameters, the model-observation discrepancies can be reduced, but the parameters become physically unrealistic.

In the present paper, a new parameterization of dust dry deposition is proposed. The deposition velocity is derived from the dust concentration equation with a boundary condition which involves the surface collection process. The relationship between surface momentum flux (drag) and deposition flux is established by combining momentum depletion and dust collection. The drag partition theory and its parameterization are introduced to describe the surface collection process in the new scheme. The effects of gravitational settling and surface collectors over a rough surface are now adequately dealt with. Finally, the new scheme is validated by the measurements of the wind-tunnel experiments as described in Zhang et al. (2014).

2 Parameterization scheme for dust deposition

2.1 Assumptions

We firstly introduce the assumptions for the new scheme. Following Raupach (1992) and Shao and Yang (2005, 2008), we consider a rough surface to be a flat ground surface superposed with roughness elements (rocks, trees, buildings etc.) as illustrated in Fig. 2a. The roughness elements are assumed to be uniform in size and randomly distributed on the surface (Fig. 2b). The flow and dust fields over the surface are in steady state and horizontally homogeneous.

The atmospheric boundary layer is divided into two parts (Fig. 3). The upper part above the collection layer is the transfer layer, in which dust is transported mainly by eddy diffusion and gravitation settling. As dust concentration is in steady state and horizontally homogeneous, the dust deposition flux, F_d, is vertically constant and obeys the following equation:

$$F_\mathrm{d} = -(k_\mathrm{p} + K_\mathrm{p}) \cdot \frac{\partial c}{\partial z} - w_\mathrm{t} \cdot c \qquad (1)$$

ACPD
14, 8063–8094, 2014

where c is dust concentration, k_p dust Brownian diffusivity, K_p dust eddy diffusivity and w_t the dust terminal velocity. F_d is upward positive.

The lower part is the collection layer with thickness of

$$h = h_c + \delta \tag{2}$$

where h_c is the roughness element height and δ the thickness of the laminar layer over the roughness elements. The laminar layer may be broken at the top of the elements and h_c is usually much larger than δ. Therefore, in general, the thickness of the collection layer is h_c for a rough surface and δ for a smooth surface.

Equation (1) can be solved for a given boundary condition. Since F_d is vertically constant and deposition velocity is defined as $w_d = -F_d/c$ (w_d is downward positive). By solving Eq. (1), one obtains that

$$w_d(z) = \left(r_g + \frac{r_s - r_g}{\exp(r_a/r_g)} \right)^{-1} \tag{3}$$

with the boundary condition

$$w_d(h) = -\frac{F_d}{c(h)} = \frac{1}{r_s} \tag{4}$$

where r_a is the aerodynamic resistance accounting for the dust diffusion, given by

$$r_a\,(z) = \int_h^z \frac{1}{K_p(z) + k_p} \mathrm{d}z \tag{5}$$

r_s is the surface collection resistance, and r_g the gravitational resistance defined as the inverse of dust terminal velocity, i.e. $r_g = w_t^{-1}$.

ACPD
14, 8063–8094, 2014

2.2 Aerodynamic resistance

In the transfer layer, k_p is negligible and K_p can be derived from the eddy viscosity for neutral particles K_T. Csanady (1963) derived an expression of the ratio of K_p/K_T (i.e. Sc_T, the turbulent Schmidt number) by taking the trajectory-crossing effect into consideration

$$Sc_T = \frac{K_p}{K_T} = \left(1 + \frac{\alpha^2 w_t^2}{\sigma^2}\right)^{-1/2} \tag{6}$$

where α is a dimensionless coefficient and σ the standard deviation of the turbulent velocity. In this study, α is taken as 1 and σ as friction velocity u_*. The expression of K_T is normally found as (Seinfeld and Pandis, 2012)

$$K_T = \frac{\kappa u_* (z - z_d)}{\varphi(\zeta)} \tag{7}$$

where k is the von Karman constant, and z_d the zero-plane displacement height, φ a stability function, $\zeta = (z - z_d)/L$ and L the Obukhov length.

An integration of Eq. (5) yields

$$r_a(z) = \frac{1}{Sc_T \cdot \kappa u_*} \left\{ \left[\varphi(\zeta) \cdot \ln(z - z_d)\right]_h^z - \int_h^z \ln(z - z_d) d(\varphi) \right\} \tag{8}$$

For neutral atmospheric boundary layers, $\varphi = 1$. Then we have

$$r_a(z) = \frac{1}{Sc_T \cdot \kappa u_*} \ln\left(\frac{z - z_d}{h_c - z_d}\right) \quad \text{for rough surface} \tag{9a}$$

$$r_a(z) = \frac{B_1}{Sc_T \cdot \kappa u_*} \ln\left(\frac{z}{z_0}\right) \quad \text{for smooth surface} \tag{9b}$$

ACPD
14, 8063–8094, 2014

where B_1 is an empirical constant determined by the airflow characteristic over the surface. The term B_1/Sc_T is set to 0.6 in SS80 and 1 in Zhang et al. (2001). In this study, the value of B_1 is estimated to be 0.45, based on the wind-tunnel measurements of Zhang et al. (2014).

2.3 Gravitational resistance

In the Stokes regime, r_g can be calculated as

$$r_g = (T_p \cdot g)^{-1} \quad (10)$$

where g is the gravitational acceleration and

$$T_p = \frac{C_c \rho_p D_p^2}{18\mu} \quad (11)$$

is the particle relaxation time. C_c the Cunningham correction factor which accounts for non-continuum effects when calculating drag on small particles, D_p particle diameter, ρ_p particle density and μ air viscosity.

2.4 Surface collection resistance

The surface collection resistance is the essence of the lower boundary condition for solving Eq. (1), which is given either in form of the deposition flux or dust concentration at the surface. As the rough surface is considered to be a smooth surface superposed with rough elements (Fig. 2), it comprises upward facing areas (ground and element roof areas) and the side areas of the elements. The deposition flux can be thus partitioned to several components which correspond to the deposition fluxes to these areas, similar to drag partition. By doing so, a relationship between the dust flux partition and drag partition can be established and the drag partition theory enables the estimation of the surface collection resistance.

ACPD
14, 8063–8094, 2014

In analogy to drag partition theory (e.g. Arya, 1975; Raupach, 1992; Shao and Yang, 2005, 2008), the deposition flux can be split into three parts:

$$F_d = F_{d,c} + F_{d,s} + F_{d,r} \tag{12}$$

where $F_{d,c}$ is the dust flux due to dust collection by the roughness elements (collectors), $F_{d,s}$ is that deposited on the ground surface and $F_{d,r}$ on the roof of the elements.

Per definition, the force exerted on a roughness element (pressure drag) can be calculated as

$$\tau_c = C_d \cdot \rho_a \cdot \lambda \cdot u_a^2(h) \tag{13}$$

where C_d, the drag coefficient for isolated roughness element, is approximately 0.3 (Shao, 2008), ρ_a air density, λ the frontal area index ($\sim d_c h_c$) of the roughness element and u_a the air horizontal speed. Similarly, the dust flux due to dust collection by the roughness elements can be expressed as

$$F_{d,c} = -E \cdot c(h) \cdot \lambda \cdot u_a(h) \tag{14}$$

where c is dust concentration and E dust collection efficiency of isolated roughness elements.

A combination of Eqs. (13) and (14) yields the relationship between the pressure drag and the deposited flux due to roughness element collection and thus the expression of $F_{d,c}$ can be written as

$$F_{d,c} = -\frac{\tau_c}{\tau} \cdot \frac{\tau}{\rho_a u_a(h)} \cdot \frac{E}{C_d} \cdot c(h) \tag{15}$$

where τ is the total shear stress (or drag) on the surface. The element collection efficiency, E, represents the collected fraction of all dust particles initially moving on a collision course with the roughness elements. It consists of the contributions of Brownian motion, impaction and interception, i.e.

$$E = E^B + E^{im} + E^{in} \tag{16}$$

ACPD
14, 8063–8094, 2014

where E^{B} is the collection efficiency caused by Brownian motion and can be estimated following Petroff et al. (2008):

$$E^{\mathrm{B}} = C_{\mathrm{B}}\mathrm{Sc}^{-2/3}Re^{n_{\mathrm{B}}-1} \quad (17)$$

where $\mathrm{Sc} = \nu/k_{\mathrm{p}}$ is the Schmidt number with ν being the kinematic viscosity and k_{p} the particle molecular diffusivity. *Re* is the roughness element Reynolds number. C_{B} and n_{B} are parameters depending on flow regimes as shown in Table 1.

E^{im} is the impaction efficiency due to dust collection on roughness elements. Following Petroff et al. (2008), we have,

$$E^{\mathrm{im}} = \left(\frac{\mathrm{St}}{0.6+\mathrm{St}}\right)^2 \quad (18)$$

where $\mathrm{St} = T_{\mathrm{p}}u_*/d_{\mathrm{c}}$.

Taking into account of the possible particle growth, $D_{\mathrm{p},\delta}$ is used to distinguish from D_{p} for describing the size of grown particles moving close to the surface. $D_{\mathrm{p},\delta}$ can be estimated following Fitzgerald (1975) or Gerber (1985). Later, the subscript δ is introduced (e.g. $T_{\mathrm{p},\delta}$) to describe the replacement of D_{p} with $D_{\mathrm{p},\delta}$ in the relevant calculations.

E^{in} is the collection efficiency due to interception. Based on the theoretical results for potential flows, Fuchs (1964) suggested that E^{in} should be directly proportional to particle size (D_{p}) and inversely proportional to the size of roughness element (d_{c}). Slinn (1982) considered that in addition to the size of the roughness element, the micro roughness characteristics (i.e. the characteristics of the roughness element surface, e.g. hair on tree leaves) are also important for interception. Our wind-tunnel study (Zhang et al., 2014) shows E^{in} is also enhanced by friction velocity, u_*. In summary, it is appropriate to propose that

$$E^{\mathrm{in}} = A_{\mathrm{in}} \cdot u_* \cdot 10^{-\mathrm{St}} \cdot \frac{2 \cdot D_{\mathrm{p},\delta}}{d_{\mathrm{c}}} \quad (19)$$

ACPD
14, 8063–8094, 2014

A new parameterization of dust dry deposition over rough surfaces

J. Zhang and Y. Shao

According to the definition, interception describes the behaviors of particles which can follow the flow well. The term $10^{-\mathrm{St}}$ is introduced to correct the deviation from this requirement, and it approaches 1 for particles of small inertial. To account for the effect of micro-roughness characteristics, the term $A_{\mathrm{in}} u_*$ is introduced, with A_{in} being an empirical parameter related to the micro-roughness characteristics, e.g., the ratio of hair size to roughness element size.

Dust deposition to the element-roof and the ground surfaces is caused by the mechanisms of gravitational settling, Brownian diffusion and impaction, thus we have

$$F_{\mathrm{d,r}} = F_{\mathrm{d,r}}^{\mathrm{g}} + F_{\mathrm{d,r}}^{\mathrm{B}} + F_{\mathrm{d,r}}^{\mathrm{im}} \tag{20}$$

$$F_{\mathrm{d,s}} = F_{\mathrm{d,s}}^{\mathrm{g}} + F_{\mathrm{d,s}}^{\mathrm{B}} + F_{\mathrm{d,s}}^{\mathrm{im}} \tag{21}$$

where $F_{\mathrm{d,r}}^{\mathrm{g}}$ and $F_{\mathrm{d,s}}^{\mathrm{g}}$ are caused by gravitational settling, $F_{\mathrm{d,r}}^{\mathrm{B}}$ and $F_{\mathrm{d,s}}^{\mathrm{B}}$ by Brownian diffusion and $F_{\mathrm{d,r}}^{\mathrm{im}}$ and $F_{\mathrm{d,s}}^{\mathrm{im}}$ by impaction.

The gravitational settling fluxes can be calculated as

$$F_{\mathrm{d,r}}^{\mathrm{g}} = -w_{\mathrm{t},\delta} \cdot c(h) \cdot \eta \tag{22}$$

$$F_{\mathrm{d,s}}^{\mathrm{g}} = -w_{\mathrm{t},\delta} \cdot c(h) \cdot (1-\eta) \tag{23}$$

where η is the basal area index (fraction of cover) of the roughness elements. The terminal velocity of dust particles near the surface, $w_{\mathrm{t},\delta}$, is calculated as

$$w_{\mathrm{t},\delta} = T_{\mathrm{p},\delta} \cdot g \tag{24}$$

Brownian diffusion is another important mechanism responsible for dust particle (especially very small particles) to move across the laminar layer. This process of dust transfer is closely related to momentum transfer. Dust particles, for which Brownian diffusion is effective, usually do not rebound from the surface (Chamberlain, 1967). For these particles, the surface dust concentration, $c(0)$, can be assumed to be zero. We

ACPD
14, 8063–8094, 2014

therefore have

$$F_{\mathrm{d,r}}^{\mathrm{B}} = -k_{\mathrm{p}} \cdot \frac{c(h)}{\delta} \cdot \eta \tag{25}$$

$$\tau_{\mathrm{r}} = \nu \cdot \frac{\rho_{\mathrm{a}} u_{\mathrm{a}}(h)}{\delta} \cdot \eta \tag{26}$$

A combination of Eqs. (25) and (26) leads to

$$F_{\mathrm{d,r}}^{\mathrm{B}} = -\frac{\tau_{\mathrm{r}}}{\rho_{\mathrm{a}} u_{\mathrm{a}}(h)} \cdot \mathrm{Sc}^{-1} \cdot c(h) \tag{27}$$

According to the drag partition theory, the drag on the ground surface is

$$\tau_{\mathrm{s}} = \tau - \tau_{\mathrm{c}} - \tau_{\mathrm{r}} \tag{28}$$

where τ is the total shear stress (or drag) on the surface, τ_{c} the pressure drag and τ_{r} the drag on the roof of the roughness elements. The pressure drag, τ_{c}, leads to a momentum reduction of the mean flow by production of turbulence, and the enhanced turbulence has a positive contribution to the Brownian diffusion over the ground surface. Further, we assume $c(\delta) = c(h)$. In analogy to Eq. (27), the deposition flux caused by Brownian diffusion to the ground surface is

$$F_{\mathrm{d,s}}^{\mathrm{B}} = -\frac{\tau + \tau_{\mathrm{c}} - \tau_{\mathrm{r}}}{\rho_{\mathrm{a}} \cdot u_{\mathrm{a}}(h)} \cdot \mathrm{Sc}^{-1} \cdot c(h) \tag{29}$$

Dust is also collected by the surfaces due to turbulent impaction. Studies show that turbulent impaction is depended on turbulence near the surface and the dimensionless particle relaxation time $T_{\mathrm{p},\delta}^{+}$. Following SS80, dust deposition due to impaction on an upward facing surface can be expressed as

$$F_{\mathrm{d,r}}^{\mathrm{im}} + F_{\mathrm{d,s}}^{\mathrm{im}} = -\frac{\tau}{\rho_{\mathrm{a}} \cdot u_{\mathrm{a}}(h)} \cdot 10^{-\frac{3}{T_{\mathrm{p},\delta}^{+}}} \cdot c(h) \tag{30}$$

ACPD
14, 8063–8094, 2014

Title Page
Abstract | Introduction
Conclusions | References
Tables | Figures
◂◂ | ▸▸
◂ | ▸
Back | Close
Full Screen / Esc
Printer-friendly Version
Interactive Discussion

where $T^+_{p,\delta}$ is defined as

$$T^+_{p,\delta} = \frac{T_{p,\delta} \cdot u_*^2}{\nu} \tag{31}$$

Finally, it follows from Eqs. (12) to (31) that

$$F_d = -\left\{ \frac{\tau}{\rho_a \cdot u_a(h)} \left[\frac{E}{C_d} \cdot \frac{\tau_c}{\tau} + \left(1 + \frac{\tau_c}{\tau}\right) \cdot \mathrm{Sc}^{-1} + 10^{-\frac{3}{T^+_{p,\delta}}} \right] + w_{t,\delta} \right\} c(h) \tag{32}$$

According to Eq. (4) and taking account of the rebound effect, the surface resistance is found to be

$$r_s = \left\{ R \cdot w_{dm} \left[\frac{E}{C_d} \cdot \frac{\tau_c}{\tau} + \left(1 + \frac{\tau_c}{\tau}\right) \cdot \mathrm{Sc}^{-1} + 10^{-\frac{3}{T^+_{p,\delta}}} \right] + w_{t,\delta} \right\}^{-1} \tag{33}$$

where

$$R = \exp\left(-b\sqrt{\mathrm{St}}\right) \tag{34}$$

with b being an empirical constant of about 2 (Chamberlain, 1967). In the studies of Giorgi (1988) and Zhang et al. (2001), b is set to 1. In Eq. (33),

$$w_{dm} = \frac{\tau}{\rho_a \cdot u_a(h_c)} \tag{35}$$

is the conductance for momentum. For smooth surfaces, w_{dm} is given by

$$w_{dm} = B_2 \cdot u_* \tag{36}$$

where B_2 is an empirical constant of about 3 (Zhang et al., 2001).

ACPD
14, 8063–8094, 2014

The term τ_c/τ can be evaluated following the drag partition formulation of Shao and Yang (2005):

$$\frac{\tau_c}{\tau} = \frac{\beta\lambda_e}{1+\beta\lambda_e} \quad (37)$$

and

$$\lambda_e = \frac{\lambda}{(1-\eta)^{c_2}} \cdot \exp\left(-\frac{c_1\lambda}{(1-\eta)^{c_2}}\right) \quad (38)$$

with $c_1 = 6$, $c_2 = 0.1$ and $\beta = 200$ which is the ratio of the pressure drag coefficient to the surface drag coefficient.

To sum up, the parameters used in the new scheme are organized and shown in Table 2. In comparison to the existing dust deposition schemes, the new scheme appears to require three additional parameters for the characterization of the rough surface, namely, h_c, λ and η (or d_c), or if the aspect ratio of the roughness elements is given two additional parameters, namely, h_c and λ. Note however z_d and z_0 used for wind profile description can be expressed following Shao and Yang (2008) in terms of h_c, λ and η. Thus, the new scheme requires only one parameter more than existing schemes. If h_c/d_c is specified, then, it requires no more parameters than the existing schemes.

3 Validation

For validation, we test the new scheme for four different surfaces studied in the wind-tunnel experiment of Zhang et al. (2014). The values of relevant parameters are listed in Table 3. The predictions of deposition velocity as a function of dust particle size are compared with the wind-tunnel measurements and the predictions using the SS80 and/or S82 schemes (Fig. 4).

For the sticky wood surface, roughness elements are absence. Dust collection is realized through impaction, Brownian motion and gravitational settling. Particle rebound does not occur for the stickiness of the surface. As shown in Fig. 4a, the new

ACPD
14, 8063–8094, 2014

scheme well predicted the wind-tunnel observations and performed better than the SS80 scheme. It should be pointed out that due to the limitations of the measurement device (a Phase Doppler Anemometry) used in the wind-tunnel experiments comparison can only be made for particles bigger than 1 µm.

The sand surface is used as the second case to test the new scheme (Fig. 4b). The difference between the sand surface and the sticky wood surface is that the presence of the sand particles (act as roughness elements, although their sizes are small) not only enhances turbulence over the surface but also improves the surface collection efficiency. In our scheme, the size of the elements is taken to be the average diameter of the sand particles and the element height half that diameter. The sand particles are assumed to be distributed uniformly on the surface and the distance between them twice the diameter. The other surface parameters, such as the frontal area and basal area indices can be calculated according to these assumptions. The rebound effect is taken into account and the *b* parameter is set to 1. As sand grains are smooth (no hair), A_{in} is set to 1.

Again, the predictions of the new scheme agree well with the experimental data (Fig. 4b). Compared with the SS80 scheme, the new scheme is obviously an improvement, especially for the particle size range 1–10 µm. The enhancement of the deposition velocity can be attributed to the better treatment of interception in the new scheme, which is neglected in the SS80 scheme. The comparison shows that even small roughness elements on a surface can play an important role in the process of dust deposition.

The third case tested is the tree surface with rather complex structures. The roughness element (tree) size is $d_c = 5$ mm and the height $h_c = 230$ mm. Taking into account the effect of leaves, we set $A_{\text{in}} = 150$ and $\lambda = 0.4$. The predictions of the new scheme shown in Fig. 4c agree well with the experimental data and are better than the results of the S82 scheme.

We also tested the new scheme for the water surface. As shown in Fig. 4d, if particle size growth (due to high humidity near the water surface) is assumed, then the predicted deposition velocity with the SS80 scheme can be made to match the experimental data. However, this good agreement is for the wrong reason: the Silicon Dioxide particles used in the experiments are not hygroscopic, to which the particle growth theory (Fitzgerald, 1975) does not apply. On the other hand, it is incorrect to treat the water surface under windy conditions as a smooth surface because of the waves, bubbles and spray droplets emitted from the surface.

The new scheme allows a better description of dust deposition on the water surface which under windy conditions can be treated as a rough surface with waves acting as roughness elements. The input parameters used in the new scheme are taken as $h_c = 30z_0$, $d_c = 0.1$ mm and the distances between the adjacent elements are supposed to be equal to h_c. The other surface parameters, including element density and frontal area index, can be computed from these parameters. Bubbles and/or spray droplets over the water surface behave like hair on tree leaves, and we therefore set $A_{in} = 100$. Using the wind field parameters derived from the wind-tunnel experiments, the deposition velocities for different particle sizes are calculated. The results shown in Fig. 5d confirm the good agreement between the scheme predictions with the experimental data. We have shown that the enhanced deposition over the water surface is indeed not due to particle growth, but due to the enhanced collection capacities of the water surface caused by waves, bubbles and spray droplets.

4 Sensitivity analysis

The main advantage of the new scheme is the improved capacity for parameterization of dust deposition to rough surfaces and the results shown in the previous section highlighted this capacity. As the scheme through comparison with the wind-tunnel observations. As the scheme performance depends on the certainty of the input parameters listed in Table 2, it is important to examine the sensitivity of the scheme to these parameters and to identify the most influential ones.

Table 2 shows that dust deposition depends on particle properties (size and density), aerodynamic conditions (friction velocity, roughness length and zero-plane dis-

ACPD
14, 8063–8094, 2014

placement) and surface characteristics (roughness element height, frontal area index and fraction of cover). These parameters are not all necessarily independent, because roughness length and zero-plane displacement are functions of the surface characteristics (Shao and Yang, 2005, 2008).

We first consider the sensitivity of dust deposition to particle properties. The typical behavior of the deposition velocity as a function of particle size is as shown in Fig. 4: it is large for small particles (< 0.01 µm) because of Brownian diffusion and is large for big particles (> 50 µm) because of gravitational settling. Dust deposition is suppressed for particles in the range from 0.01 to 50 µm, because they are too big for Brownian diffusion and too small for gravitational settling. Normally, the minimum deposition velocity occurs in the range from 0.1 to 1 µm (Fig. 4a and b), but the enhancement of interception shifts this range to smaller particles (Fig. 4c and d).

Particle density influences gravitational settling and the processes related to particle inertia, such as impaction. As shown in Fig. 5a, the variability of particle density mainly affects the deposition of particles larger than 5 µm via the modification of gravitational settling.

We now examine the sensitivity of the scheme to aerodynamic parameters. Friction velocity is an aerodynamic parameter which influences the entire deposition process from turbulent diffusion to surface collection. As shown in Fig. 5b, the influence of u_* is predominantly for particles smaller than 10 µm, for which the deposition depends strongly on turbulent diffusion. An increased friction velocity also improves the surface collection due to impaction and interception and hence results in a noticeable enhancement of deposition for particles between 0.1 and 10 µm.

Finally, we consider the sensitivity of the scheme to surface characteristics. Roughness element size affects the element collection efficiency and two parameters are used to describe the element size in the new scheme. One is element diameter, d_c, and the other the micro-roughness parameter, A_{in}. Micro-roughness features, such as hair on the element, enhance the element collection efficiency due to interception (Chamberlain, 1967; S82). For smooth elements ($A_{in} = 1$), the influence of d_c can be

Discussion Paper | Discussion Paper | Discussion Paper | Discussion Paper |

ACPD
14, 8063–8094, 2014

A new parameterization of dust dry deposition over rough surfaces

J. Zhang and Y. Shao

readily analyzed. As Fig. 5c shows, d_c mainly affects the deposition of particles in the size range of 0.1 to 10 µm, because it determines the collection efficiency due to impaction and interception. For particles in the range of 0.1 to 5 µm, deposition velocity is increased for small element size because of the improved interception. For particles from 5 to 50 µm, impaction increases with element size and so does deposition velocity.

While d_c is usually too large to affect interception, the influence of A_{in} is significant and most profound on the deposition of particles in the size range of 0.1 to 10 µm (Fig. 5d).

The parameter R describes the rebound probability when a particle collides with the surface. The influence of R on the deposition is visible for coarse particles larger than 5 µm (Fig. 5e).

Roughness element frontal area index is a parameter used to describe the element distribution on the surface, used in the drag partition theory. We now test its influence on dust deposition. As shown in Fig. 5f, deposition velocity first increases, then decreases with frontal area index. The influence is apparent for particles of all sizes, especially for particles in the range of 0.1 to 1 µm. Figure 5f suggests that in case of small frontal area index, the roughness elements make the surface rougher and enhance the surface collection, but as the number of roughness elements further increases, the surface becomes again smoother and the surface collection efficiency is decreased. The influences of element frontal area index on surface resistance and deposition velocity for particles with diameter 1 µm are shown in Fig. 6.

5 Summary and discussion

A new dust deposition scheme is proposed by taking into account the impact of roughness elements on turbulent diffusion and surface collection. The relationship between the aerodynamics and surface collection process is established, and the effect of the roughness elements on dust deposition is incorporated in the scheme by using the

ACPD
14, 8063–8094, 2014

analogy of deposition flux partition to drag partition. Also, a modified expression for interception is proposed to account for the micro-roughness effect of the elements.

The new scheme has been tested against the wind-tunnel experimental data and good agreement between the scheme predictions and the observations is achieved. A new and more realistic explanation based on the new scheme is proposed for the enhanced dust deposition over water surfaces, i.e., water surface under windy conditions should be treated as a rough surface due to waves and spray droplets. We have however not yet validated the scheme against field observations. As wind-tunnel data have limitations due to simple turbulence and simple surface conditions, we cannot claim that the scheme is sufficiently thoroughly tested. Also, we do not claim that our scheme is superior to the existing schemes, such as those of Zhang et al. (2001), Petroff and Zhang (2010), Kouznetsov and Sofiev (2012) etc. It appears desirable to do a thorough comparison with the other existing schemes, together with the other model developers, against a reliable field dataset.

The sensitivity of the new scheme to some of the important input parameters has been tested. It is found that dust density and particle rebound probability mostly influence the deposition of coarse particles larger than 5 µm; the size and micro-roughness characteristics of the roughness elements influence interception noticeably and hence the deposition of particles in the size range of 0.1 to 10 µm; friction velocity affects the entire deposition process and influences the deposition of particles of all sizes; element frontal area index has a predominant effect on surface collection efficiency and influences the deposition of particles of all sizes.

While we believe the new scheme has improved the capacity for parameterizing dust deposition over rough surfaces, some questions remain unanswered and future research is required in the following areas.

The effect of wind intermittency: in our study, we assumed the wind is steady and the effect of wind intermittency is neglected. But wind intermittency may have a significant effect on dust deposition, including dust transport in the upper layer and dust collection in the lower layer (Fig. 3). While some studies on the topic already exist, e.g.,

ACPD
14, 8063–8094, 2014

the treatment of the effect of wind intermittency on aerodynamic resistance by Zhang et al. (2001) and Seinfeld and Pandis (2012), the influence of wind intermittency on the dust collection process deserves further research.

Deposition on complex surfaces: only surfaces with relatively simple and uniform elements are tested in our study, but natural surfaces are much more complex. For example, how to predict dust deposition to surfaces with multi-size roughness elements is important for regional and global dust models.

Effect of element-interaction on element collection efficiency: in analogy to the drag partition theory, an expression for describing the distribution of total deposited dust on different parts of the surface (elements or upward facing surface) has been proposed in our study. But the element collection efficiency is evaluated based on the study of isolated elements. The effect on element collection efficiency due to the interactions between the roughness elements remains rather unclear.

Acknowledgements. This work is supported by the DFG (Deutsche Forschungsgemeinschaft) project "A Wind-tunnel Study on Dust-deposition Mechanisms and Validation of Dust-deposition Schemes", Natural Science Foundation of China (Project 11172118) and the Innovative Research Groups of the National Natural Science Foundation of China (Project 11121202).

References

Arya, S. P. S.: A drag partition theory for determining the large-scale roughness parameter and wind stress on the Arctic pack ice, J. Geophys. Res., 80, 3447–3454, 1975.

Chamberlain, A. C.: Transport of Lycopodium spores and other small particles to rough surfaces, P. Roy. Soc. Lond. A Mat., 296, 45–70, 1967.

Csanady, G. T.: Turbulent diffusion of heavy particles in the atmosphere, J. Atmos. Sci., 20, 201–208, 1963.

Droppo, J. G.: Improved Formulations for Air-Surface Exchanges Related to National Security Needs: Dry Deposition Models, Pacific Northwest National Laboratory, Richland, WA, 2006.

Fitzgerald, J. W.: Approximation formulas for the equilibrium size of an aerosol particle as a function of its dry size and composition and the ambient relative humidity, J. Appl. Meteorol., 14, 1044–1049, 1975.
Fuchs, N. A.: Mechanics of Aerosols, Pergamon, New York, 1964.
Gerber, H. E.: Relative-humidity parameterization of the Navy Aerosol Model (NAM) (No. NRL-8956), Naval Research Lab, Washington DC, 1985.
Giorgi, F.: Dry deposition velocities of atmospheric aerosols as inferred by applying a particle dry deposition parameterization to a general circulation model, Tellus B, 40, 23–41, 1988.
Hicks, B. B., Baldocchi, D. D., Meyers, T. P., Hosker Jr., R. P., and Matt, D. R.: A preliminary multiple resistance routine for deriving dry deposition velocities from measured quantities, Water Air Soil Poll., 36, 311–330, 1987.
Kouznetsov, R. and Sofiev, M.: A methodology for evaluation of vertical dispersion and dry deposition of atmospheric aerosols, J. Geophys. Res., 117, D01202, doi:10.1029/2011JD016366, 2010.
Petroff, A., Mailliat, A., Amielh, M., and Anselmet, F.: Aerosol dry deposition on vegetative canopies, Part II: A new modelling approach and applications, Atmos. Environ., 42, 3654–3683, 2008.
Petroff, A. and Zhang, L.: Development and validation of a size-resolved particle dry deposition scheme for application in aerosol transport models, Geosci. Model Dev., 3, 753–769, doi:10.5194/gmd-3-753-2010, 2010.
Raupach, M.: Drag and drag partition on rough surfaces, Bound.-Lay. Meteorol., 60, 375–395, 1992.
Raupach, M. R., Briggs, P. R., Ford, P. W., Ahmad, N., and Edge, V. E.: Endosulfan transport: II. Modeling airborne dispersal and deposition by spray and vapor, J. Environ. Qual., 30, 729–740, 2001.
Sehmel, G. A.: Particle and gas dry deposition: a review, Atmos. Environ., 14, 983–1011, 1980.
Seinfeld, J. H. and Pandis, S. N.: Atmospheric Chemistry and Physics: From Air Pollution to Climate Change, John Wiley, New York, 2012.
Shao, Y.: Physics and Modelling of Wind Erosion, 2 edn., Springer, Berlin, 2008.
Shao, Y. and Yang, Y.: A scheme for drag partition over rough surfaces, Atmos. Environ., 39, 7351–7361, 2005.
Shao, Y. and Yang, Y.: A theory of drag partition over rough surfaces, J. Geophys. Res., 113, F02S05, doi:10.1029/2007JF000791, 2008.

ACPD
14, 8063–8094, 2014

A new parameterization of dust dry deposition over rough surfaces

J. Zhang and Y. Shao

Slinn, W. G. N.: Predictions for particle deposition to vegetative canopies, Atmos. Environ., 16, 1785–1794, 1982.
Slinn, S. A. and Slinn, W. G. N.: Predictions for particle deposition on natural waters, Atmos. Environ., 14, 1013–1016, 1980.
Venkatram, A. and Pleim, J.: The electrical analogy does not apply to modeling dry deposition of particles, Atmos. Environ., 33, 3075–3076, 1999.
Wesely, M. L. and Hicks, B. B.: A review of the current status of knowledge on dry deposition, Atmos. Environ., 34, 2261–2282, 2000.
Zhang, L., Gong, S., Padro, J., and Barrie, L.: A size-segregated particle dry deposition scheme for an atmospheric aerosol module, Atmos. Environ., 35, 549–560, 2001.
Zhang, J., Shao, Y., and Huang, N.: Measurements of Dust Deposition Velocity in a Wind-Tunnel Experiment, 2014 (companion paper).

ACPD
14, 8063–8094, 2014

A new parameterization of dust dry deposition over rough surfaces

J. Zhang and Y. Shao

Table 1. Typical values of C_B and n_B in Eq. (17) for different Reynolds numbers (Petroff et al., 2008).

Re	C_B	n_B
$1–4 \times 10^3$	0.467	1/2
$4 \times 10^3–4 \times 10^4$	0.203	3/5
$4 \times 10^4–4 \times 10^5$	0.025	4/5

ACPD
14, 8063–8094, 2014

Table 2. Summary of the new dust deposition scheme and the scheme input parameters. According to the drag partition theory, z_0 and z_d which are not considered as input parameters can be estimated from surface parameters and u_* (Shao and Yang, 2005, 2008). The particle density is considered as a constant ($2200\,\mathrm{kg\,m^{-3}}$) in this study.

<table>
<tr><th colspan="7">Parameterization</th></tr>
<tr><td>Wind field</td><td colspan="4">Surface</td><td colspan="2">Particle</td></tr>
<tr><td>u_*</td><td>h_c</td><td>d_c</td><td>λ</td><td>A_m</td><td>b</td><td>D_p</td></tr>
<tr><td colspan="2">Rough surface</td><td rowspan="5">$\frac{\tau_c}{\tau} = f(n,\lambda,\eta)$
Drag partition</td><td rowspan="5">$E = E^B + E^{im} + E^{in}$
Element collection</td><td rowspan="5">$D_{p,\delta}$
Particle growth</td><td rowspan="5">R
Rebound</td><td rowspan="5">$r_g = \frac{18\mu}{C_c \rho_p D_p^2 g}$
Settling resistance</td></tr>
<tr><td>$r_a(z) = \frac{1}{Sc_T \cdot \kappa \cdot u_*} \ln\left(\frac{z - z_d}{h_c - z_d}\right)$</td><td>$w_{dm} = \frac{u_*^2}{u_a(h_c)}$</td></tr>
<tr><td colspan="2">Smooth surface</td></tr>
<tr><td>$r_a(z) = \frac{B_1}{Sc_T \cdot \kappa \cdot u_*} \cdot \ln\left(\frac{z}{z_0}\right)$</td><td>$w_{dm} = B_2 \cdot u_*$</td></tr>
<tr><td>$B_1 = 0.45$</td><td>$B_2 = 3$</td></tr>
<tr><td colspan="7">$$r_s = \left\{ R \cdot w_{dm} \left[\frac{E}{C_d} \cdot \frac{\tau_c}{\tau} + \left(1 + \frac{\tau_c}{\tau}\right) \cdot Sc^{-1} + 10^{-\frac{3}{\tau_p^+}} \right] + w_{t,\delta} \right\}^{-1}$$</td></tr>
<tr><td colspan="7">$$w_d(z) = \left(r_g + \frac{r_s - r_g}{\exp\left(r_a / r_g\right)} \right)^{-1}$$</td></tr>
</table>

ACPD
14, 8063–8094, 2014

J. Zhang and Y. Shao

Table 3. Parameters for validation of the new scheme for the four different surfaces studied in the wind-tunnel experiments of Zhang et al. (2014). For all tests, particle density $\rho_p = 2200\,\mathrm{kg\,m^{-3}}$ is used. The wind parameters are obtained from the experimental data.

	z_r (mm)	u_* ($\mathrm{m\,s^{-1}}$)	z_0 (mm)	z_d (mm)	h_c (mm)	d_c (mm)	λ	A_{in}	b
Sticky wood	15	0.12	0.075	0	0	0	0	1	0
		0.40	0.033	0	0	0	0	1	0
		0.54	0.032	0	0	0	0	1	0
Sand	15	0.14	0.153	0	0.2	0.1	0.125	1	1
		0.32	0.143	0	0.2	0.1	0.125	1	1
		0.49	0.135	0	0.2	0.1	0.125	1	1
Tree	250	0.24	5.927	200	230	5	0.4	150	0.01
		0.50	2.877	200	230	5	0.4	150	0.01
		1.06	2.106	200	230	5	0.4	150	0.01
Water	25	0.15	0.300	0	$30z_0$	0.1	0.538	100	0
		0.36	0.306	0	$30z_0$	0.1	0.538	100	0
		0.57	0.309	0	$30z_0$	0.1	0.538	100	0

ACPD
14, 8063–8094, 2014

A new parameterization of dust dry deposition over rough surfaces

J. Zhang and Y. Shao

Table A1. List of symbols.

A_{in}	Empirical parameter for surface micro-roughness characteristics	–
B_1, B_2	Empirical constant	–
b	Numerical constant in rebound expression	–
c	Dust concentration	$kg\,m^{-3}$
C_c	Cunningham correction factor	–
C_d	Drag coefficient for obstacle	–
D_p, $D_{p,\delta}$	Dry/wet particle diameter	m
d_c, d_c^l, d_c^s	Dimension of the roughness elements, large collector (i.e. roughness elements) and small collector	m
E, E^B, E^{in}, E^{im}	Element collection efficiency for different mechanisms	–
F_d	Dust deposition flux	$kg\,m^{-2}\,s^{-1}$
g	Gravitational acceleration	$m\,s^{-2}$
h	Thickness of surface collection layer	m
h_c	Height of roughness element	m
K_B	Boltzmann constant	$J\,K^{-1}$
K_p	Particle eddy diffusivity	$m^2\,s^{-1}$
K_T	Turbulent (or eddy) viscosity	$m^2\,s^{-1}$
k_p	Brownian diffusion coefficient	$m^2\,s^{-1}$
R	Reduction in collection caused by rebound	–
Re	Reynolds number	–
r_a	Aerodynamic resistance	$s\,m^{-1}$
r_s	Surface collection resistance	$s\,m^{-1}$
r_g	Resistance of gravity (inverse of terminal velocity)	$s\,m^{-1}$
Sc	Schmidt number	–
Sc_T	Turbulent Schmidt number	–

ACPD
14, 8063–8094, 2014

Table A1. Continued.

St	Stokes number	–
T_p	Relaxation time of particle	s
T_p^+	Dimensionless particle relaxation time	–
u_a	Horizontal velocity of air	$m s^{-1}$
u_*	Friction velocity	$m s^{-1}$
w_d	Deposition velocity $w_d = -F_d/C$	$m s^{-1}$
w_t	Terminal velocity	$m s^{-1}$
z, z_r	Height and reference height	m
z_0, z_d	Roughness length and zero-plane displacement	m
	Greek symbols	
β	Ratio of the drag coefficient for isolated roughness element to that for bare surface, evaluated to 200 in this study	–
δ	Thickness of laminar layer	m
η	Basal area index	–
κ	von Karman constant	–
λ	Frontal area index	–
μ	Dynamic viscosity of air	$kg m^{-1} s^{-1}$
ν	Kinematic viscosity of air	$m^2 s^{-1}$
ρ_p, ρ_a	Particle/air density	$kg m^{-3}$
τ, τ_c, τ_s, τ_r	Drag exerted on different parts of the surface	$N m^{-2}$

ACPD
14, 8063–8094, 2014

A new parameterization of dust dry deposition over rough surfaces

J. Zhang and Y. Shao

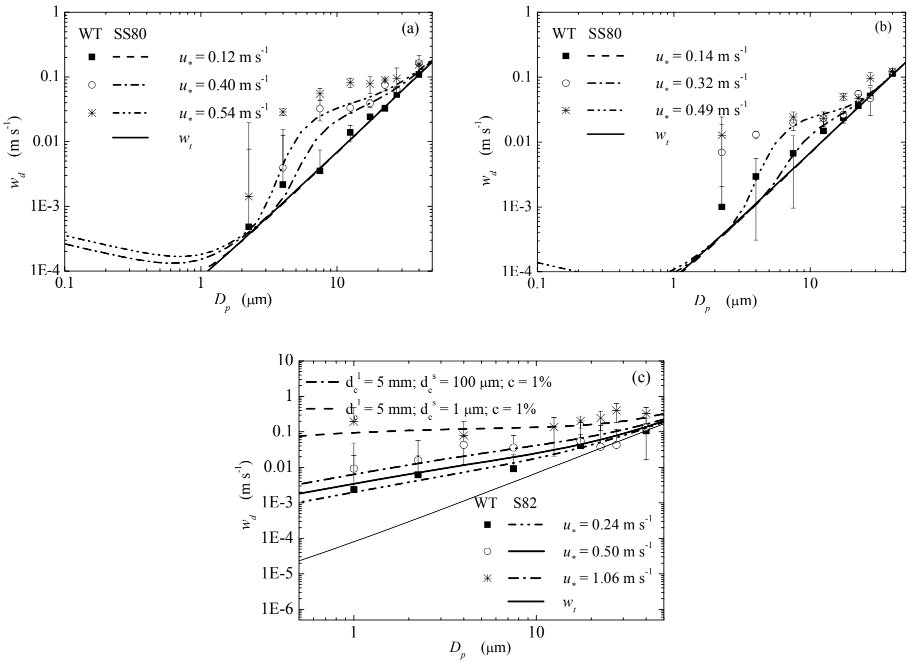

Fig. 1. Comparison of deposition velocity predicted by the SS80 and S82 schemes (lines) with the wind-tunnel measurements (symbols) over three different surfaces. **(a)** Sticky wood; **(b)** Sand; **(c)** Tree.

ACPD
14, 8063–8094, 2014

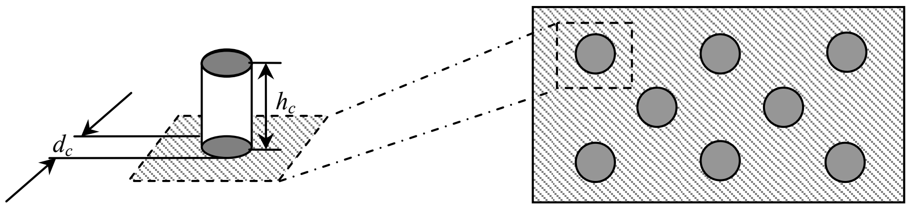

(a) Roughness element

(b) Top view of rough surface

Fig. 2. Illustration of rough surface. **(a)** A roughness element with height h_c and diameter d_c; **(b)** Roughness elements randomly distributed on the surface.

ACPD
14, 8063–8094, 2014

A new parameterization of dust dry deposition over rough surfaces

J. Zhang and Y. Shao

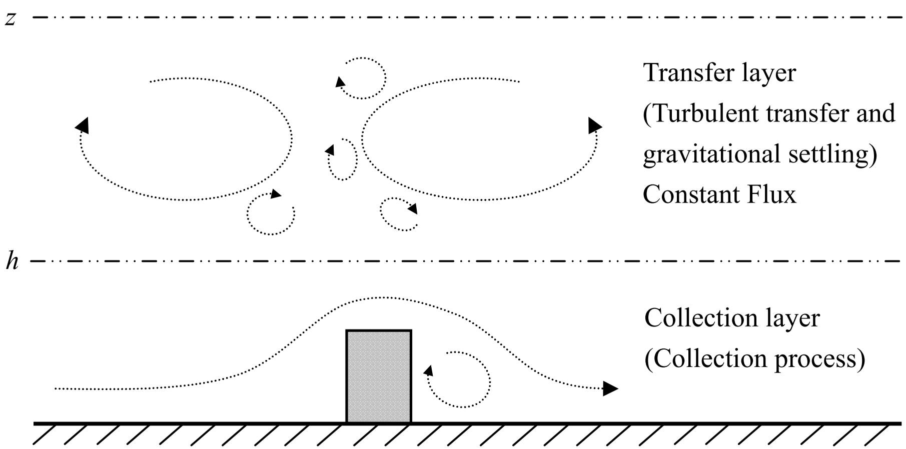

Fig. 3. Illustration of the two-layer model. The lower layer, from the ground to the top of the laminar (or quasi-laminar) layer, is the collection layer where the dust collection process takes place. Over the collection layer is the transfer layer, where turbulent transfer and gravitational settling are dominant and the dust flux is vertically constant. Air flow is represented by the dash lines.

ACPD
14, 8063–8094, 2014

A new parameterization of dust dry deposition over rough surfaces

J. Zhang and Y. Shao

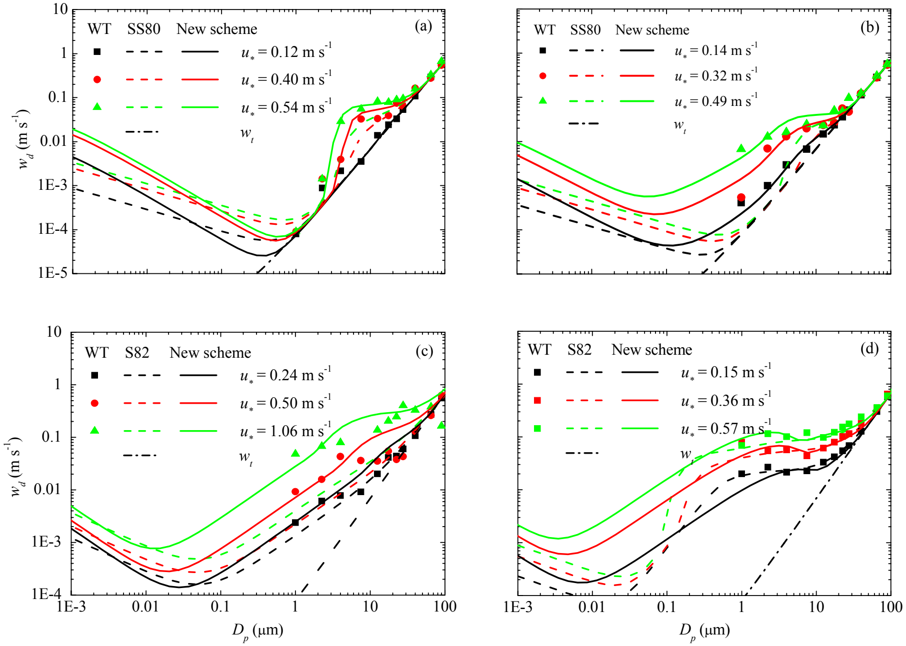

Fig. 4. Comparison of deposition velocity, w_d, as a function of particle diameter, D_p, predicted by the new scheme (solid lines) and the SS80 or S82 scheme (dashed lines) with the wind-tunnel (WT) measurements (symbols) for the **(a)** sticky wood, **(b)** sand, **(c)** tree and **(d)** water surface.

ACPD
14, 8063–8094, 2014

A new parameterization of dust dry deposition over rough surfaces

J. Zhang and Y. Shao

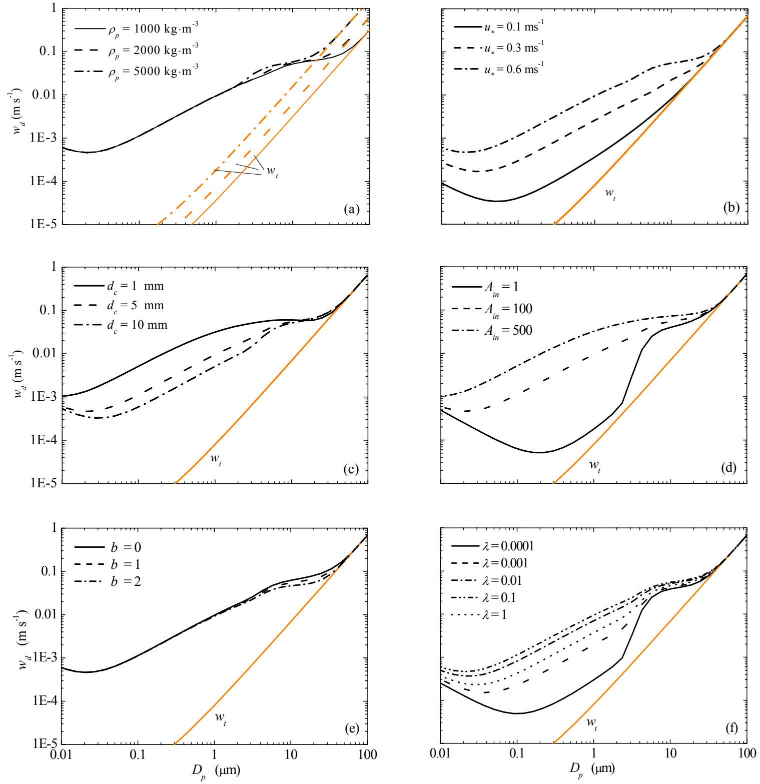

Fig. 5. Sensitivity of deposition velocity to **(a)** particle density, **(b)** friction velocity, **(c)** roughness element size, **(d)** surface micro-roughness, **(e)** rebound probability and **(f)** element frontal area index. The deposition velocity is calculated for the reference height 1 m and the relevant parameter is evaluated as follows unless otherwise stated: $\rho_p = 2200\,\mathrm{kg\,m^{-3}}$, $u_* = 0.6\,\mathrm{m\,s^{-1}}$, $z_0 = 10\,\mathrm{mm}$, $z_d = 100\,\mathrm{mm}$, $h_c = 150\,\mathrm{mm}$, $d_c = 5\,\mathrm{mm}$, $A_{in} = 100$, $b = 1$ and $\lambda = 0.1$.

ACPD
14, 8063–8094, 2014

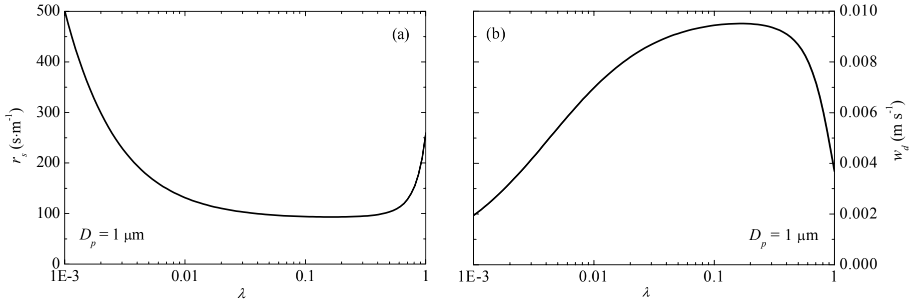

Fig. 6. The influence of element frontal area index on **(a)** surface resistance and **(b)** deposition velocity for particles with diameter of 1 µm. The relevant parameters are the same as for Fig. 5.

ACPD
14, 8063–8094, 2014